Radboud Repository

Radboud University Nijmegen

PDF hosted at the Radboud Repository of the Radboud University Nijmegen

The following full text is a publisher's version.

For additional information about this publication click this link.
http://hdl.handle.net/2066/201985

Please be advised that this information was generated on 2021-01-23 and may be subject to change.

Journal of Molecular Structure 1184 (2019) 139–145

Contents lists available at ScienceDirect

Journal of Molecular Structure

journal homepage: http://www.elsevier.com/locate/molstruc

Structural changes upon electronic excitation in 1,2-dimethoxybenzene from rotationally resolved electronic spectroscopy of various isotopologues

Marie-Luise Hebestreit [a], Christian Henrichs [a], Michael Schneider [a], Martin Wilke [a], W. Leo Meerts [b], Daniel Krügler [c], Michael Schmitt [a, *]

[a] Heinrich-Heine-Universität, Institut für Physikalische Chemie I, D-40225 Düsseldorf, Germany
[b] Radboud University, Institute for Molecules and Materials, Felix Laboratory, Toernooiveld 7c, 6525 ED Nijmegen, the Netherlands
[c] Bruker-Daltonik GmbH, 28359 Bremen, Germany

ARTICLE INFO

Article history:
Received 23 October 2018
Received in revised form
11 December 2018
Accepted 24 January 2019
Available online 5 February 2019

Keywords:
Dimethoxybenzene
High resolution electronic spectroscopy
Rotational constants
ab initio
Pseudo-Kraitchman
Evolutionary algorithms

ABSTRACT

The structural changes of 1,2-dimethoxybenzene upon electronic excitation have been elucidated from a comparison of *ab initio* calculations and fits of the structural changes to experimental inertial parameters both in the basis of internal coordinates as well as in vibrational distortion coordinates. It is shown that the use of vibrational distortion coordinates leads to better agreement with the results of *ab initio* optimized structures compared to the use of internal coordinates in cases, that the inertial data are not sufficient for a complete structure determination. 1,2-dimethoxybenzene has been found to be only very slightly *ortho*-quinoidally distorted upon electronic excitation, in contrast to former expectations.

© 2019 The Authors. Published by Elsevier B.V. This is an open access article under the CC BY-NC-ND license (http://creativecommons.org/licenses/by-nc-nd/4.0/).

1. Introduction

Structural changes of disubstituted benzenes upon electronic excitation reflect the altered electron densities in the excited state. Substituents can have different electronic effects with respect to the aromatic ring. They either push electrons into the ring via inductive (+I) or mesomeric (+M) effects or, they draw electrons via inductive (−I) or mesomeric (−M) effects. While for molecules in their electronic ground state, this is standard textbook knowledge, the relative strengths of these effects are strongly dependent on the electronic state. In the present study, we investigate the effect of two methoxy substituents in different conformers of dimethoxybenzene (DMB) on the geometry change of the benzene ring upon electronic excitation.

Molecular beam R2PI spectra of 1,2-, 1,3-, and 1,4-dihydroxybenzene (catechol, resorcinol, and benzoquinone) have been reported by Dunn et al., from which they concluded the existence of two rotamers for 1,4-dihydroxybenzene and of three rotamers for 1,2- and 1,3-dihydroxybenzene, respectively [1]. Bürgi and Leutwyler studied 1,2-dihydroxybenzene (catechol), using hole-burning spectroscopy [2]. They found, that all bands in the vibronic spectrum belong to a single rotamer. Myszkiewicz et al. presented a study on 1,3-dihydroxybenzene (resorcinol), using rotationally resolved laser induced fluorescence spectroscopy [3]. Only two rotamers could be identified in the molecular beam spectra of 1,3-dihydroxybenzene. Two 1,4-dihydroxybenzene (benzoquinone) rotamers have been studied at rotational resolution in the group of Pratt and the two origins were assigned to the *cis* and *trans* rotamers on the basis of their different nuclear spin statistical weights and the different rotational constants [4].

Huang et al. [5] measured the vibrational spectrum of 1,2-dimethoxybenzene (1,2-DMB) in the S_1 and in the D_0 states and found only one conformer in the resonant two-color ionization spectrum. A high resolution study of 1,2-DMB and its water cluster has been performed in the Pratt group [6]. They could show, that all bands in the vibronic spectrum have the same rotational constants in the ground state and belong therefore to the same rotamer,

---

* Corresponding author.
E-mail addresses: mschmitt@uni-duesseldorf.de, mschmitt@hhu.de (M. Schmitt).

https://doi.org/10.1016/j.molstruc.2019.01.074
0022-2860/© 2019 The Authors. Published by Elsevier B.V. This is an open access article under the CC BY-NC-ND license (http://creativecommons.org/licenses/by-nc-nd/4.0/).

which was identified from a comparison to quantum chemical calculations as the *trans*-1,2-DMB rotamer. The dipole moments of several rotamers of 1,2-, 1,3-, and 1,4-DMB have been studied by Schneider et al. using rotationally resolved electronic Stark spectroscopy [7].

In the present contribution, we determine the structural changes of several rotamers of 1,2-DMB from the fits of rotational constants of several isotopologues.

2. Computational methods

2.1. Quantum chemical calculations

Structure optimizations were performed employing Dunning's correlation consistent polarized valence triple zeta (cc-pVTZ) basis set from the TURBOMOLE library [8,9]. The equilibrium geometries of the electronic ground and the lowest excited singlet states were optimized using the approximate coupled cluster singles and doubles model (CC2) employing the resolution-of-the-identity approximation (RI) [10–12]. Anharmonic normal mode analyses have been performed to compute vibrational averaging effect on the inertial defects of the molecules under consideration. Such an anharmonic analysis is implemented in the Gaussian program package [13]. The procedure for the calculation of cubic and of some of the quartic force constants utilizes numerical derivatives of the analytically determined Hessian with respect to the normal coordinates. We performed the analysis for the electronic ground state with density functional theory (DFT), employing the B3LYP functional with the 6-311G (d,p) basis set, and for the excited state using time-dependent DFT with the same functional and basis set.

2.2. Fits of the rovibronic spectra using evolutionary algorithms

Evolutionary algorithms have proven to be perfect tools for the automated fit of rotationally resolved spectra, even for large molecules and dense spectra [14–17]. Beside a correct Hamiltonian to describe the spectrum and reliable intensities inside the spectrum, an appropriate search method is needed. Evolutionary strategies are powerful tools to handle complex multi-parameter optimizations and find the global optimum. For the analysis of the presented high-resolution spectra we used the covariance matrix adaptation evolution strategy (CMA-ES), which is described in detail elsewhere [18,19]. In this variant of global optimizers mutations are adapted via a covariance matrix adaptation (CMA) mechanism to find the global minimum even on rugged search landscapes that are additionally complicated due to noise, local minima and/or sharp bends.

2.3. Fits of the structural changes upon electronic excitation

2.3.1. Structure fit in internal coordinates

Structural parameters of the molecules are fit to the rotational constants in each of the electronic states using the program *pKrFit* [20]. Due to the limited number of inertial parameters only vibrationally zero-point averaged structural parameters, r_0 were fit. These r_0 structures depend on the isotopomers, as has been shown by Costain [21]. The fit was performed in internal coordinates using a non-linear Levenberg-Marquart variant [22,23]. The fit target is to find the set of internal coordinates which gives the closest agreement between the measured and the calculated rotational constants of all isotopologues. Additional linear constraints among the internal parameters could be defined to be used in the minimization procedure. The advantage of the use of internal coordinates is, that they implicitly fulfill the three center-of-mass and the three vanishing products-of-inertia conditions and that it is relatively easy to define additional linear constraints among these coordinates [20,24]. Subsequently, the geometry changes upon electronic excitation are obtained as differences of the individually fitted structural parameters. Additionally, a global minimizer, based on genetic algorithms (GA) [25] has been used, which allows intermediate local minimization steps rather than simple cost function evaluations [26]. This technique was originally introduced by Li and Scheraga as part of a simulated annealing (SA) exploration of the potential hypersurface of proteins [27]. Also known as *basin-hopping* [28] by Doyle and Wales, it was successfully combined with GA and SA to determine minimum-energy structures of fullerene and atomic clusters [29–32].

2.3.2. Structure fit in vibrational displacement coordinates

A second approach uses linear combinations of normal modes as basis for the geometry changes upon excitation. The *ab initio* optimized ground state geometry is distorted along selected normal modes, whose scaling factors are fit to the differences of the rotational constants in the ground and electronically excited state using the program *FCFit* [33]. The Hessians and geometries of both electronic states connected by the transition were obtained from a normal mode analysis at the CC2/cc-pVTZ optimized structures using numerical second derivatives of the potential energy from the NumForce script in TURBOMOLE. This approach has the advantage to directly yield geometry changes from the rotational constants changes without the need of fitting the geometries of both states independently. The success of the method however, depends on a meaningful selection of the normal modes, which are the basis for the geometry changes.

3. Experimental methods

1,2-Dimethoxybenzene ($\geq$ 99%) was purchased from Sigma-Aldrich and used without further purification. 1,2-Dimethoxybenzene-d6 (complete deuteration of both CH_3 groups) was purchased from CDN Isotopes.

For the high resolution laser induced fluorescence (HRLIF) spectra, the samples were heated to 60 °C and co-expanded with 200–300 mbar of argon into the vacuum through a cylindrical 200 μm nozzle. After the expansion a molecular beam was formed using two skimmers (1 mm and 3 mm, 330 mm apart) linearly aligned inside a differentially pumped vacuum system consisting of three vacuum chambers. The molecular beam was crossed at right angles with the laser beam 360 mm downstream of the nozzle. To create the excitation beam, 10 W of the 532 nm line of a diode pumped solid state laser (Spectra-Physics Millennia eV) pumped a single frequency ring dye laser (Sirah Matisse DS) operated with Rhodamine 110. The light of the dye laser was frequency doubled in an external folded ring cavity (Spectra Physics Wavetrain) with a resulting power of about 5 mW during the experiments. The fluorescence of the samples was collected perpendicular to the plane defined by laser and molecular beam using an imaging optics setup consisting of a concave mirror and two plano-convex lenses onto the photocathode of an UV enhanced photomultiplier tube (Thorn EMI 9863QB). The signal output was then discriminated and digitized by a photon counter and transmitted to a PC for data recording and processing. The relative frequency was determined with a *quasi* confocal Fabry-Perot interferometer. The absolute frequency was obtained by comparing the recorded spectrum to the tabulated lines in the iodine absorption spectrum [34]. A detailed description of the experimental setup for the rotationally resolved laser induced fluorescence spectroscopy has been given previously [35,36].

4. Results

4.1. Computational results

The nomenclature for the rotamers we adopt here, refers to the dihedral angles of the methoxy groups with respect to the aromatic plane. The numbering starts at the lowest number in the benzene ring, at the position adjacent to the first substituent. For the first rotamer of 1,2-DMB in Fig. 1 the first dihedral angle formed by C (2) C (1)O (7)C (9) is 180°, the second by C (3)C (2)O (8)C (10) is 0°. Thus, the labeling for this rotamer is (180/0). The second rotamer has a dihedral angle C (2)C (1)O (7)C (9) of 0° and C (3)C (2)O (8)C (10) of 0°, therefore named (0/0).

The (180/0) rotamer of 1,2-DMB is the only stable planar rotamer. Its structure was optimized at the CC2/cc-pVTZ level of theory in the S_0 and the lowest excited singlet state S_1. The Cartesian coordinates of all stable structures are given in the online supporting material.

4.2. Symmetries and nuclear spin statistical considerations

Rotamer (180/0) of 1,2-DMB has the point group symmetry C_{2v}. Considering the internal rotational degrees of freedom of the methyl rotors in the two equivalent methoxy groups, it belongs to the molecular symmetry group G36. Since the barrier to methyl rotation is so high, that the subtorsional splitting is not observed experimentally, we will go on with the (rigid) C_{2v} point group and regard internal rotation as not feasible under our experimental conditions. Rotamer (180/0) has five pairs of equivalent protons: three pairs from the methyl groups and two pairs at position 3/6 and 4/5 of the benzene ring. These ten protons give rise to a total of 1024 nuclear spin functions (2^{10}), which are divided into 528 symmetric and 496 antisymmetric nuclear spin functions.[1] They can be reduced to 33 symmetric and 31 antisymmetric nuclear spin functions. The symmetry axis for the interchange of the five pairs of identical protons in rotamer (180/0) of 1,2-DMB is the molecular *b*-axis (cf. Fig. 1).

The methyl-deuterated isotopologue of 1,2-DMB has two pairs of identical protons and three pairs of identical deuterons. The number of symmetric spin functions (S_1) due to the equivalent protons is 10, and for the antisymmetric spin function (A_1) 6. The number symmetric spin functions for the three pairs of deuterons (S_2), which are bosons with $I = 1$, is 378, and for the antisymmetric spin functions (A_2) is 351. Combining the spin functions for the protons and deuterons results in $S_1 \cdot S_2 + A_1 \cdot A_2 = 5886$ symmetric and $S_1 \cdot A_2 + S_2 \cdot A_1 = 5778$ antisymmetric spin functions, which can be reduced to 109 symmetric and 107 antisymmetric spin functions.

The total wave function, which is the product of the nuclear spin function, the vibrational, the electronic and the rotational wave function must be antisymmetric with respect to the rotation about the *b*-axis. The electronic and vibrational wave functions are totally symmetric, so the only symmetry we have to consider is that of the rotational wave functions. The rotational wave functions symmetric to C_2^b which are determined from the rotational Four group symmetries are (ee) and (oo) for K_a and K_c, the antisymmetric wave functions are (eo) and (oe), respectively [37].

Thus, for five equivalent protons, the rotational states with even product of K_aK_c symmetries have a spin statistical weight of 31, odd K_aK_c levels of 33, those with two equivalent protons and three equivalent deuterons with even product of K_aK_c symmetries have a spin statistical weight of 107, odd K_aK_c levels of 109, cf. Table 1.

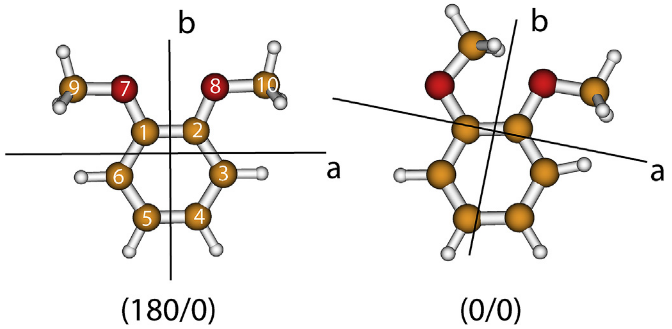

Fig. 1. Structures of the two possible rotamers of 1,2-DMB with their principal inertial axes.

Table 1
Symmetries and spin statistical weights of the rotational wave functions for the rotamers of 1,2-DMB.

K_aK_c	h_{10}	d_6
ee	31	107
oo	31	107
oe	33	109
eo	33	109

The spin statistical weights for the different deuterated dimethoxybenzenes can be obtained similarly and are given in Table 1.

4.3. Experimental results

4.3.1. Rotationally resolved electronic spectra of 1,2-DMB isotopologues

Fig. 2 shows the rotationally resolved electronic spectra of the origin bands of h_{10}-1,2-DMB and of d_6-1,2-DMB. The fit of the h_{10}-1,2-DMB could be improved, by taking the correct nuclear spin statistical weights of 31 for the levels with even (odd) K_a and even (odd) K_c and of 33 for levels with odd (even) K_a and even (odd) K_c. This variation of 6% is easily detectable for the h_{10} isotopologue. For the d_6 isotopologue, the difference of nuclear spin weights of 107 for ee and oo levels and of 109 for eo and oe levels is too small to cause a difference in the quality of the fit. Table 2 gives the inertial parameters for both isotopologues, their theoretically predicted values from the CC2/cc-pVTZ optimized structures and their differences. All isotopic shifts are accurately predicted, both for the ground and the excited state. These values will later on be used for the determination of structural changes upon electronic excitation. The shift of +14 cm^{-1} of the electronic origin of d_6-1,2-DMB with respect to h_{10}-1,2-DMB is considerably larger than twice the shift of d_3-methoxybenzene with respect to methoxybenzene (+3 cm^{-1}) [38]. We therefore conclude that a vibrational interaction between the two methyl rotors takes place in 1,2-DMB, not surprising, regarding their neighboring position in the benzene ring.

5. Discussion

5.1. Geometric structures

5.1.1. Inertial defects

1,2-DMB has a planar heavy atom structure, as can be inferred

---

[1] The number of symmetric spin functions for *n* pairs of identical nuclei with Spin $I = 1/2$ is given by Ref. [37]: $N_{sym} = \frac{1}{2}[\prod_{i=1}^{n}(2I_i+1)][\prod_{i=1}^{n}(2I_i+1)+1]$ and for antisymmetric spin functions by: $N_{antisym} = \frac{1}{2}[\prod_{i=1}^{n}(2I_i+1)][\prod_{i=1}^{n}(2I_i+1)-1]$.

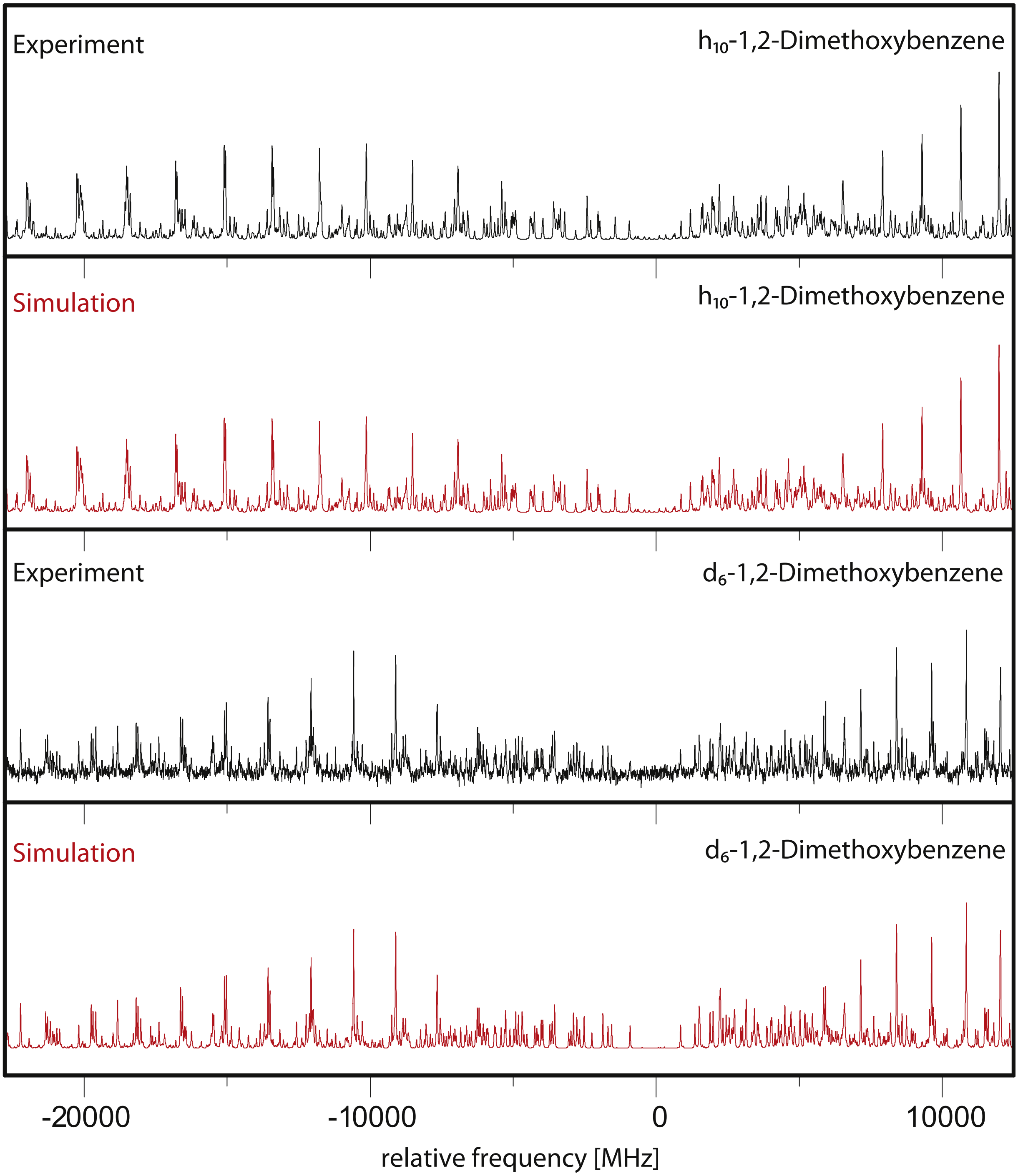

Fig. 2. Rotationally resolved electronic spectrum of the electronic origin band of h_{10}-1,2-DMB and of d_6-1,2-DMB.

from the inertial defects.[2] The ground state inertial defect of methoxybenzene (anisole) was determined to be −3.409 amu Å^2 using microwave spectroscopy [39] and in the electronically excited state to be −3.584 amu Å^2 by rotationally resolved laser induced fluorescence spectroscopy [40]. The *ab initio* calculated inertial defects at the equilibrium structures that are given in Table 2 are approximately twice as large, as the values of anisole. The inertial defect in the electronically excited state is slightly more negative than in the ground state, which can be attributed to an increased contribution of out-of-plane vibrations in the excited state. These vibrational contributions can be quantified by an anharmonic normal mode analysis that allows for the determination of vibrational averaging effects on the rotational constants and on the inertial defects [41]. These corrections have been performed with the Gaussian program package at the MP2/6-311G (d,p) level of theory. The zero-point vibrationally averaged inertial defects (at the r_0 geometries) are given along with the equilibrium inertial defects (at the r_e geometries) in Table 3 and are compared to the

---

[2] The inertial defect is defined as $I_c - I_a - I_b$, where the I_g are the moments of inertia with respect to the main inertial axes g of the molecule.

Table 2
Calculated and experimental rotational constants of 1,2-DMB isotopologues and the respective isomeric shifts Δ(Iso). Double primed parameters belong to the electronic ground and single primed to the excited state. θ is the angle of the transition dipole moment with the main inertial *a*-axis. A positive sign of this angle means a clockwise rotation of the dipole moment vector onto the main inertial *a*-axis.

	h_{10}		d_6		Δ(Iso)	
	theory	exp.	theory	exp.	theory	exp.
A''/MHz	1679	1663.1 (1)	1585	1569.1 (1)	−94	−94.0
B''/MHz	1348	1349.8 (1)	1162	1162.2 (1)	−186	−187.7
C''/MHz	755	752.6 (1)	682	679.6 (1)	−73	−73.0
$\Delta I''$ /amu Å^2	−6.40	−6.80	−12.78	−13.24	−6.38	−6.44
A'/MHz	1658	1641.6 (1)	1563	1547.2 (1)	−95	−94.4
B'/MHz	1322	1329.1 (1)	1143	1147.2 (1)	−179	181.9
C'/MHz	742	742.7 (1)	671	671.1 (1)	−71	−71.6
$\Delta I'$/amu Å^2	−6.42	−7.68	−12.82	−14.12	−6.40	−6.44
θ/°	90	90	90	90	0	0
ν_0/cm^{-1}	37884	35751	–	35765	–	+14

Table 3
Experimental inertial defects ΔI_{exp} in amu Å^2 along with the computed equilibrium ΔI_e and zero-point averaged ΔI_0 inertial defects of rotamers of 1,2-DMB.

	ΔI_{exp}	ΔI_e	ΔI_0
S_0	−6.80	−6.32	−6.80
S_1	−7.68	−9.40	−9.73
$S_0 - S_1$	−0.88	−3.08	−2.93

experimental values.

A quite large effect on the inertial defect upon electronic excitation is found for 1,2-DMB, in which the experimental inertial defect ΔI_{exp} increases from −6.80 amu Å^2 to −7.68 amu Å^2. Inspection of the equilibrium inertial defects ΔI_e in Table 3 shows that this effect can be attributed to an out-of-plane distortion of the equilibrium position of the heavy atoms of 1,2-DMB. Vibrational zero-point averaging (ΔI_0) even decreases the non-planarity of the excited state slightly.

5.1.2. Ab initio determination of geometry changes upon electronic excitation

Fig. 3b shows the changes of the relevant bond lengths in pm upon electronic excitation as obtained from the CC2/cc-pVTZ calculations. For 1,2-DMB there is a weak indication of a quinoidal distortion upon electronic excitation. The CC bonds adjacent to the OCH_3 groups expand by 5.8 pm., while those in the neighboring positions only expand by 1.0 pm. Surprisingly, the CC bond between the OCH_3 substituents contracts slightly (−0.1 pm.). Both $C_{aromatic}O$ bond distances decrease by −0.4 pm., while the OC_{methyl} bond lengths increase by 0.9 pm. Altogether, these geometry changes point to a partial localization of the CC double bonds in the aromatic ring after electronic excitation.

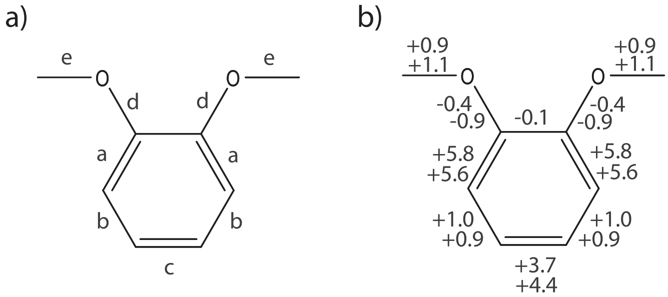

Fig. 3. a) Model parameters to be fit, using internal coordinates in the program pKrFit. b) Geometry changes in pm upon electronic excitation obtained from the CC2/cc-pVTZ optimized structures (upper numbers) and from the results of the fit using model FCFit (lower numbers). The bond length change C1C2 is not defined in the Z-matrix of the internal coordinates. Therefore, we give only the *ab initio* value.

5.1.3. Experimental determination of geometry changes upon electronic excitation

The structures of 1,2-DMB have been obtained from fits of model geometries to the experimentally determined rotational constants of two isotopologues, in internal coordinates using the program pKrFit [20] and in displacement coordinates, using the program FCFit [33]. In the following we will compare the two methods for fitting structural parameters with a limited set of inertial data.

Fit in internal coordinates For the fit of structural parameters to an incomplete set of inertial data, some constraints to the geometry have to be imposed. In principal a fit of the structure of an *N*-atomic molecule in internal coordinates requires $3N - 6$ inertial parameters from the experiment. Assuming planarity, the number of required internal coordinates reduces to $2N - 3$. Due to the symmetry plane of 1,2-DMB $N - 2$ internal coordinates are sufficient for a complete structure determination. This can be accomplished by 18 inertial parameters, i.e. five different isotopologues. Since only six rotational constants from two isotopologues are available for 1,2-DMB, a strongly simplified model for the geometry fits in internal coordinates using several geometry constraints had to be adopted. All CCC and CCH angles in the aromatic ring have been set to 120°, the CH bond lengths to the phenol values of 108 pm. in the S_0 and of 107 pm. in the S_1 state [20]. For the aromatic ring CC bond lengths three different values, designated by *a*, *b*, and *c* in Fig. 3a, are admitted, both $C_{aromatic}O$ bond lengths are set equal to *d* and both OC_{methyl} bond lengths are set to a common value *e* and fit.

The Z-matrix definition of the internal coordinates for the fit is given in the online supporting material (Table S1). Inspection of the correlation matrix of the fitted geometry parameters in Table S2 of the online supporting shows, that most of the chosen geometry parameters are uncorrelated in the fit. However, the C2C3 bond length is strongly correlated with the C2O8C10 angle and C3C4 is correlated with the bond length O8C10. These correlations can only be removed using more isotopologues.

This procedure has to be performed for the structure in the electronic ground and excited state, respectively. The structural changes upon electronic excitation are then obtained from the differences of the respective internal coordinates. The results of these fits are shown in Table 4 and compared to the values obtained from the *ab initio* calculations. We employed both a local optimizer, which is based on a non-linear Levenberg-Marquart variant, and a global optimizer, which utilizes a genetic algorithm approach. The general trends for the bond lengths are in fair agreement with the values of the *ab initio* calculations, with the global optimizer performing slightly better. However, for small changes of the structural parameters, even the sign of the change might be wrong.

Fit in vibrational distortion coordinates An alternative way to obtain the structural changes is a fit of the changes of the inertial

Table 4
Structural parameters from the *ab initio* (CC2/cc-pVTZ) calculations and the fits in displacement coordinates (using FCFit) and in internal coordinates (using pKrFit). For the definition of the structural parameters Δ*a*, Δ*b*, Δ*c*, Δ*d*, and Δ*e*, c.f. Fig. 3.

	Δ*a*	Δ*b*	Δ*c*	Δ*d*	Δ*e*
ab initio	+ 5.8	+ 1.0	+ 3.7	− 0.4	+ 0.9
FCFit (local)	+ 5.6	+ 0.9	+ 4.4	− 0.9	+ 1.1
FCFit (global)	+ 5.6	+ 0.8	+ 4.3	− 1.0	+ 1.1
pKrFit (local)	+ 2.9	− 0.2	+ 8.0	+ 0.2	+ 1.0
pKrFit (global)	+ 2.3	+ 0.5	+ 6.2	− 0.3	+ 0.8

parameters upon excitation to the changes of the structure, directly. This requires a starting structure on which the structural changes are imposed. We chose the *ab initio* structure for the ground state, which has the best agreement with the rotational constants. In our case, this is the CC2/cc-pVTZ optimized geometry. As basis for the changes of bond lengths and bond angles we chose in this case a linear combination of normal modes. These normal modes have been obtained for the ground and the excited states from the numerical second derivatives of the total energy (the molecular Hessian), which are used in a routine fashion anyhow, to confirm that the optimized structures are minima. The vibrational modes of the electronically excited state can be expressed in terms of the ground state modes using the following linear orthogonal transformation, first given by Duschinsky [42]:

$$Q' = SQ'' + d \tag{1}$$

Here, Q' and Q'' are the N-dimensional vectors of the normal modes of excited and ground state, respectively, S is a $N \times N$ rotation matrix (the Duschinsky matrix) and d is an N-dimensional vector which describes the linear displacements of the normal coordinates. The modes, which have been used as basis for the geometry change upon excitation are shown in Figure S1 of the online supporting material. As in the case of the fits in internal coordinates, we performed a local and a global fit, using the same algorithms. The results are collected in Table 4. Here, the agreement between the *ab initio* determined changes and the experimental ones is very good.

5.2. Electronic structure

As has already been stated by Yi et al., the electronic origin of 1,2-DMB is mainly of LUMO ← HOMO character [6]. From the excitation scheme, using the frontier orbitals, they deduced an *ortho*-quinoidal structure in the electronically excited state. According to our CC2 calculations, the transition has two main components: 0.89 (LUMO ← HOMO) −0.40 (LUMO +1 ← HOMO - 1), cf. Figure S2 of the online supporting material.

To rationalize the experimentally observed structural changes of 1,2-DMB, we compare them to the electron density difference plot, shown in Fig. 4. The regions, which are shown in red, have a reduction of electron density upon excitation, while those in blue have an increased electron density. Interestingly, the change of electron density in the π-space is opposite to that in the σ-space.

A strong reduction of π electron density at the oxygen atoms of the methoxy groups is accompanied by an increase of π electron density in the aromatic ring. Carbon atoms C1, C2, C3, and C6 show a large increase of π electron density, while the π density at carbon atoms C4 and C5 remain unchanged. Electron density in the bonds decreases strongly between C2 and C3 and to a lesser extent between C4 and C5. The strong increase of electron density between C1 and C2 explains nicely, why this bond length even decreases upon electronic excitation. All these findings nicely match the bond length variations upon electronic excitation as determined by the fit using vibrational distortion coordinates.

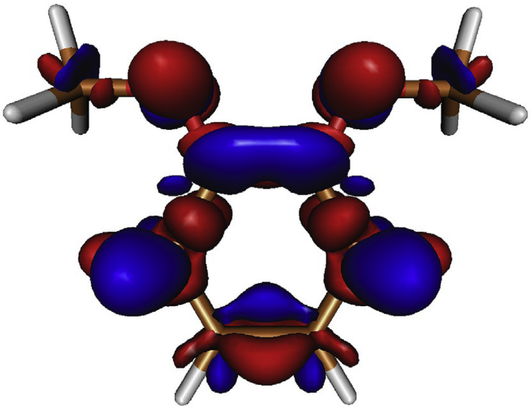

Fig. 4. Electron density difference plot for the $S_1 \leftarrow S_0$ transition of 1,2-DMB from the CC2/cc-pVTZ optimized structures for both states. Regions of decreasing electron density are shown in red, those of increasing electron density in blue.

6. Conclusions

The fit of geometry changes upon electronic excitation to the rotational constants in each state, using a *pseudo*-Kraitchman approach in internal coordinates and subsequent subtraction of the respective coordinates, leads to less reliable values, than the direct fit to the differences of the rotational constants using vibrational distortion coordinates. While the number of isotopologues, which are needed for a complete structure determination are the same for both methods, the latter has an obvious advantage in the case of insufficient inertial data. While for a fit in internal coordinates, the number of isotopologues has to be increased in order to reduce the parameter correlations, a fit in vibrational distortion coordinates opens the way to introduce independent structural informations that can be used in the fit, such as the intensities of fluorescence emission bands, whose intensity is governed by the Franck-Condon principle and therefore depends on the geometry changes.

The structural change of 12-DMB has only a slight *ortho*-quinoidal character. For the determination of bond lengths changes, the σ-electron densities are nearly as important as the π-electron densities. Considering only the frontier orbitals (π), will lead to a wrong picture of expected geometry changes.

Acknowledgements

Financial support of the Deutsche Forschungsgemeinschaft via grant SCHM1043 12-3 is gratefully acknowledged. Computational support and infrastructure was provided by the "Center for Information and Media Technology" (ZIM) at the Heinrich-Heine-University Düsseldorf. We furthermore thank the Regional Computing Center of the University of Cologne (RRZK) for providing computing time on the DFG-funded High Performance Computing (HPC) system CHEOPS as well as support.

Appendix A. Supplementary data

Supplementary data to this article can be found online at https://doi.org/10.1016/j.molstruc.2019.01.074.

References

[1] T.M. Dunn, R. Tembreull, D.M. Lubman, Chem. Phys. Lett. 121 (1985) 453–457.
[2] T. Bürgi, S. Leutwyler, J. Chem. Phys. 101 (1994) 8418–8429.
[3] G. Myszkiewicz, W.L. Meerts, C. Ratzer, M. Schmitt, ChemPhysChem 6 (2005) 2129–2136.
[4] S.J. Humphrey, D.W. Pratt, J. Chem. Phys. 99 (1993) 5078–5086.
[5] J.-H. Huang, W.-B. Tzeng, K.-L. Huang, Chin. J. Chem. 26 (2008) 51–54.
[6] J.T. Yi, J.W. Ribblett, D.W. Pratt, J. Phys. Chem. A 109 (2011) 9456–9464.
[7] M. Schneider, M. Wilke, M.-L. Hebestreit, C. Henrichs, W.L. Meerts, M. Schmitt, ChemPhysChem 19 (2018) 307–318.
[8] R. Ahlrichs, M. Bär, M. Häser, H. Horn, C. Kölmel, Chem. Phys. Lett. 162 (1989) 165–169.
[9] J.T.H. Dunning, J. Chem. Phys. 90 (1989) 1007–1023.
[10] C. Hättig, F. Weigend, J. Chem. Phys. 113 (2000) 5154–5161.
[11] C. Hättig, A. Köhn, J. Chem. Phys. 117 (2002) 6939–6951.
[12] C. Hättig, J. Chem. Phys. 118 (2002) 7751–7761.
[13] M.J. Frisch, G.W. Trucks, H.B. Schlegel, G.E. Scuseria, M.A. Robb, J.R. Cheeseman, J.A. Montgomery Jr., T. Vreven, K.N. Kudin, J.C. Burant,

J.M. Millam, S.S. Iyengar, J. Tomasi, V. Barone, B. Mennucci, M. Cossi, G. Scalmani, N. Rega, G.A. Petersson, H. Nakatsuji, M. Hada, M. Ehara, K. Toyota, R. Fukuda, J. Hasegawa, M. Ishida, T. Nakajima, Y. Honda, O. Kitao, H. Nakai, M. Klene, X. Li, J.E. Knox, H.P. Hratchian, J.B. Cross, C. Adamo, J. Jaramillo, R. Gomperts, R.E. Stratmann, O. Yazyev, A.J. Austin, R. Cammi, C. Pomelli, J.W. Ochterski, P.Y. Ayala, K. Morokuma, G.A. Voth, P. Salvador, J.J. Dannenberg, V.G. Zakrzewski, S. Dapprich, A.D. Daniels, M.C. Strain, O. Farkas, D.K. Malick, A.D. Rabuck, K. Raghavachari, J.B. Foresman, J.V. Ortiz, Q. Cui, A.G. Baboul, S. Clifford, J. Cioslowski, B.B. Stefanov, G. Liu, A. Liashenko, P. Piskorz, I. Komaromi, R.L. Martin, D.J. Fox, T. Keith, M.A. Al-Laham, C.Y. Peng, A. Nanayakkara, M. Challacombe, P.M.W. Gill, B. Johnson, W. Chen, M.W. Wong, C. Gonzalez, J.A. Pople, Gaussian 03, Revision A.1, Gaussian, Inc., Pittsburgh, PA, 2003.

[14] W.L. Meerts, M. Schmitt, G. Groenenboom, Can. J. Chem. 82 (2004) 804–819.

[15] W.L. Meerts, M. Schmitt, Phys. Scripta 73 (2005) C47–C52.

[16] W.L. Meerts, M. Schmitt, Int. Rev. Phys. Chem. 25 (2006) 353–406.

[17] M. Schmitt, W.L. Meerts, Handbook of High Resolution Spectroscopy, John Wiley and Sons, 2011.

[18] A. Ostermeier, A. Gawelcyk, N. Hansen, Parallel Problem Solving from Nature, PPSN III, Springer, Berlin/Heidelberg, 1994.

[19] N. Hansen, A. Ostermeier, Evol. Comput. 9 (2001) 159–195.

[20] C. Ratzer, J. Küpper, D. Spangenberg, M. Schmitt, Chem. Phys. 283 (2002) 153–169.

[21] C. Costain, J. Chem. Phys. 29 (1958) 864.

[22] K. Levenberg, Q. Appl. Math. Meth. 2 (1944) 164–168.

[23] D.D. Marquardt, J. Soc. Ind. Appl. Math. 11 (1963) 431–441.

[24] M. Schmitt, M. Böhm, C. Ratzer, D. Krügler, K. Kleinermanns, I. Kalkman, G. Berden, W.L. Meerts, ChemPhysChem 7 (2006) 1241–1249.

[25] D. Levine, PGAPack V1.0, PGAPack can be Obtained via Anonymous Ftp from, 1996. ftp://ftp.mcs.anl.gov/pub/pgapack/pgapack.tar.Z.

[26] M. Schmitt, D. Krügler, M. Böhm, C. Ratzer, V. Bednarska, I. Kalkman, W.L. Meerts, Phys. Chem. Chem. Phys. 8 (2006) 228–235.

[27] Z.Q. Li, H.A. Scheraga, Proc. Natl. Acad. Sci. U.S.A. 84 (1987) 6611–6615.

[28] D.J. Wales, J.P.K. Doye, J. Phys. Chem. A 101 (1998) 5111–5116.

[29] D.M. Deaven, K.M. Ho, Phys. Rev. Lett. 75 (1995) 288–291.

[30] S.K. Gregurick, M.H. Alexander, B. Hartke, J. Chem. Phys. 104 (1996) 2684–2691.

[31] J.A. Niesse, H.R. Mayne, J. Chem. Phys. 105 (1996) 4700–4706.

[32] D.M. Deaven, N. Tit, J.R. Morris, K.M. Ho, Chem. Phys. Lett. 256 (1996) 155–200.

[33] R. Brause, M. Schmitt, D. Spangenberg, K. Kleinermanns, Mol. Phys. 102 (2004) 1615–1623.

[34] S. Gerstenkorn, P. Luc, Atlas du spectre d'absorption de la molécule d'iode 14800–20000 cm^{-1}, CNRS, Paris, 1986.

[35] Habilitation M. Schmitt, Math. Nat. Fakultät, Heinrich-Heine-Universität, Düsseldorf, 2000.

[36] M. Schmitt, J. Küpper, D. Spangenberg, A. Westphal, Chem. Phys. 254 (2000) 349–361.

[37] C.H. Townes, A.L. Schawlow, Microwave Spectroscopy, Dover Publications, New York, 1975.

[38] M.M. Lindic, M. Zajonz, M.-L. Hebestreit, M. Schneider, W.L. Meerts, M. Schmitt, J. Photochem. Photobiol. A 365 (2018) 213–219.

[39] O. Desyatnyk, L. Pszczolkowski, S. Thorwirth, T.M. Krygowskid, Z. Kisiel, Phys. Chem. Chem. Phys. 7 (2005) 1708–1715.

[40] J.W. Ribblett, W.E. Sinclair, D.R. Borst, J.T. Yi, D.W. Pratt, J. Phys. Chem. A 110 (2006) 1478–1483.

[41] V. Barone, J. Chem. Phys. 122 (2005) 014108-1–014108-10.

[42] F. Duschinsky, Acta Physicochim. U.R.S.S. 7 (1937) 551–577.